Electronic Supplementary Information (ESI)

A Thermodynamic Approach toward Selective and Reversible Sub-ppm H_2S Sensing by Ultra-small CuO Nanorods impregnated with Nb_2O_5 Nanoparticles

Rahul Purbia[a], Yeong Min Kwon[b], Sung Yeol Choi[a], Sang Heon Kim[a], Yun Sik Lee[c], Zehra Betül Ahi[d], Hyesung Park[b], Jeong Min Baik[a]**

[a]School of Advanced Materials Science and Engineering, Sungkyunkwan University (SKKU) 2066 Seoburo, Suwon 16419, South Korea
[b]School of Materials Science and Engineering, Ulsan National Institute of Science and Technology (UNIST), Ulsan, 44919, Republic of Korea.
[c]School of Electrical and Computer Engineering, Ulsan National Institute of Science and Technology (UNIST), Ulsan, 44919, Republic of Korea.
[d]Pimsa Otomotive, Mahallesi, 14.Sokak No:B/1, Cayirova/Kocaeli, Turkey.

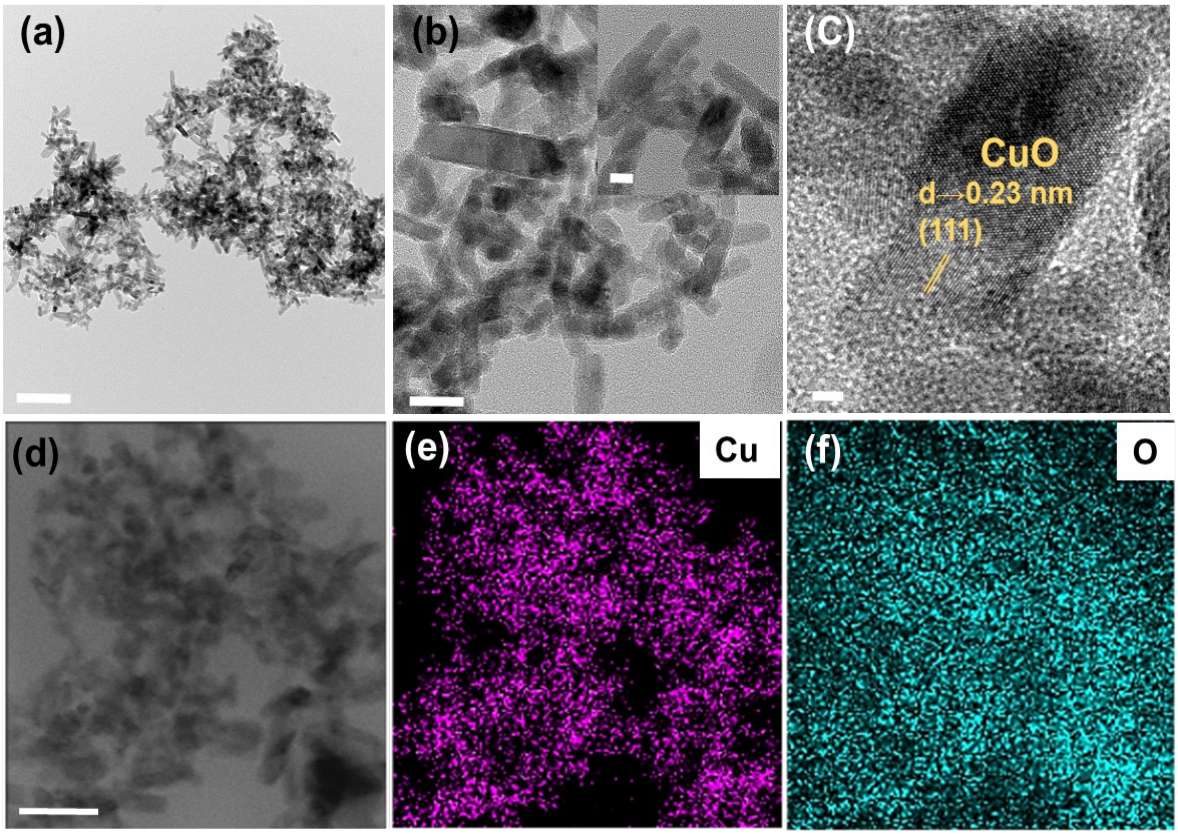

Figure S1: (a) TEM, (b-c) HR-TEM images of CuO NPs. STEM-EDS mapping images and element distribution of CuO NPs: (d) region of mapping and (e) Cu, and (f) O element distributions. (scale bar: (a) 100 nm, (b) 20 nm (inset 10 nm), (c) 2 nm, (d-f) 50 nm)

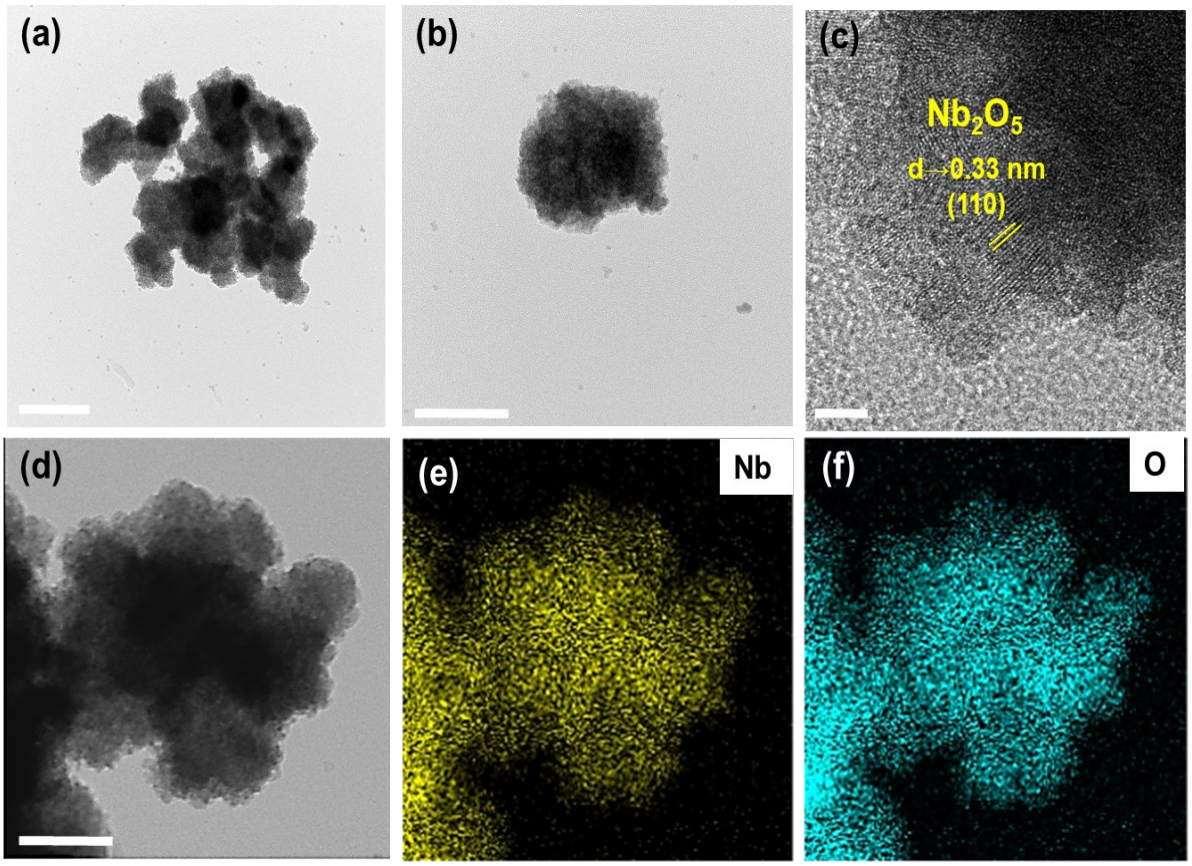

Figure S2: (a) TEM, (b-c) HR-TEM images of Nb_2O_5 NPs. STEM-EDS mapping images and element distribution of Nb_2O_5 NPs: (d) region of mapping and (e) Nb, and (f) O element distributions. (scale bar: (a) 200 nm, (b) 100 nm, (c) 5 nm, (d-f) 100 nm)

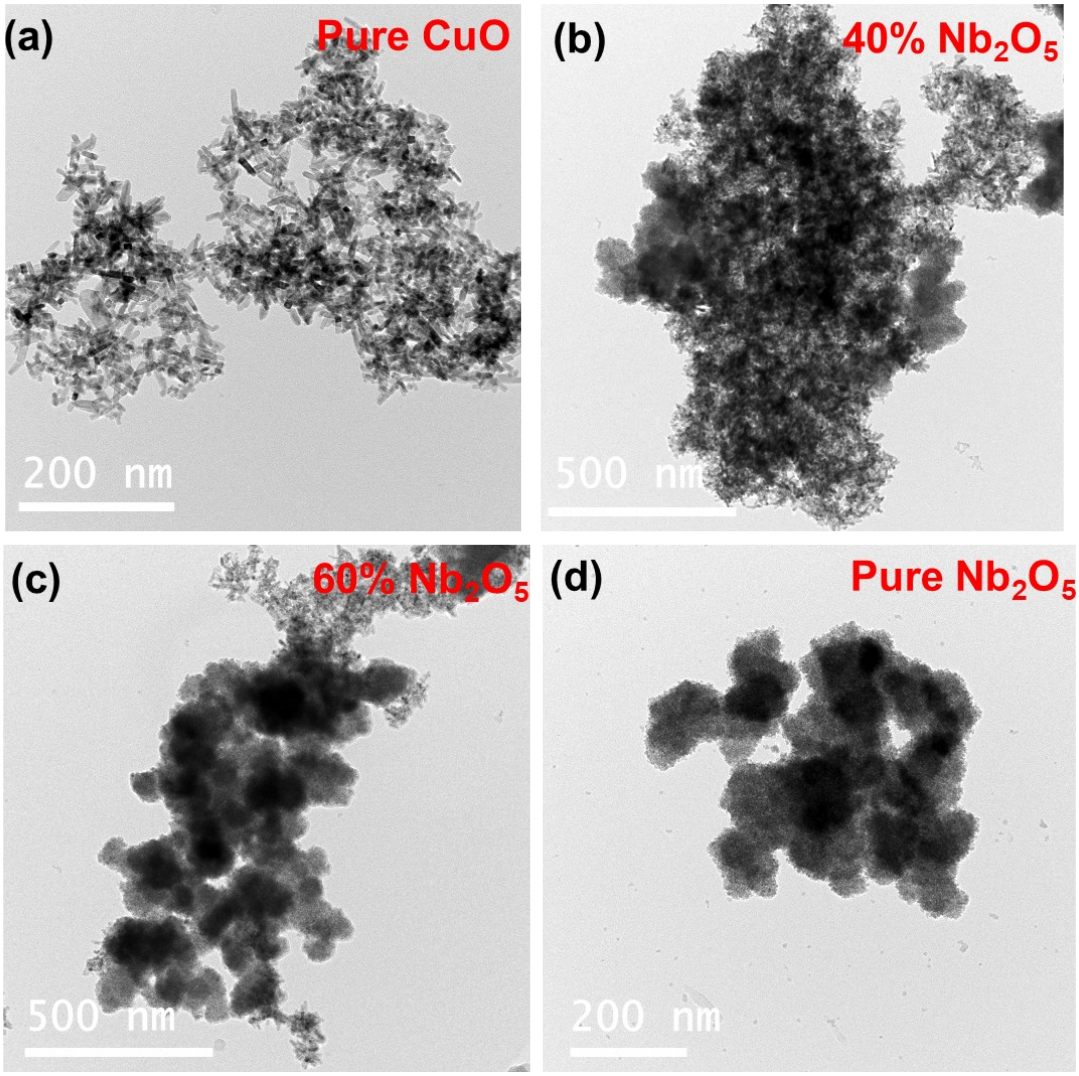

Figure S3: TEM images of composites with different concentrations of Nb_2O_5.

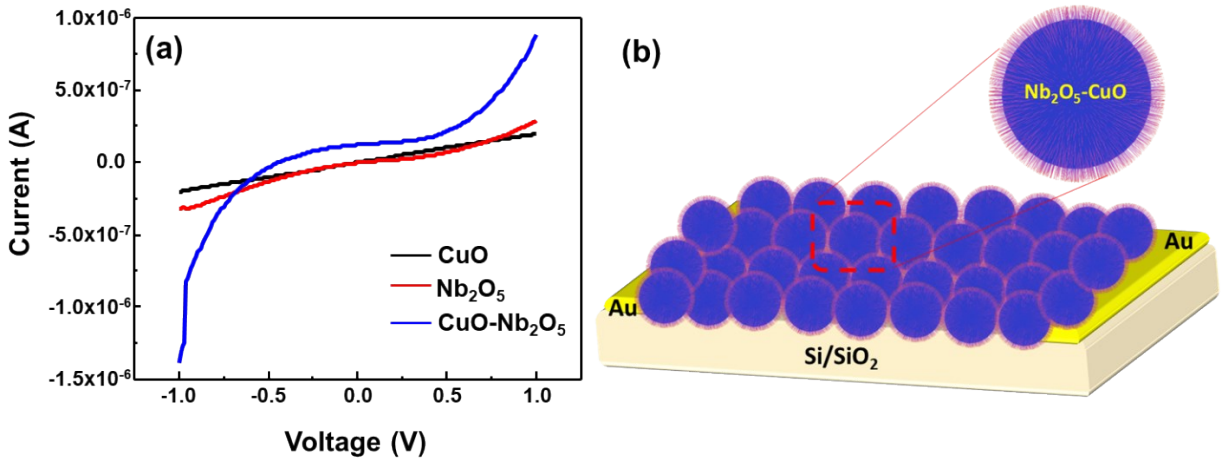

Figure S4: (a) I-V characteristics of pristine CuO, pristine Nb_2O_5, and CuO- Nb_2O_5 at room temperature (b) schematic CuO-Nb_2O_5 interface.

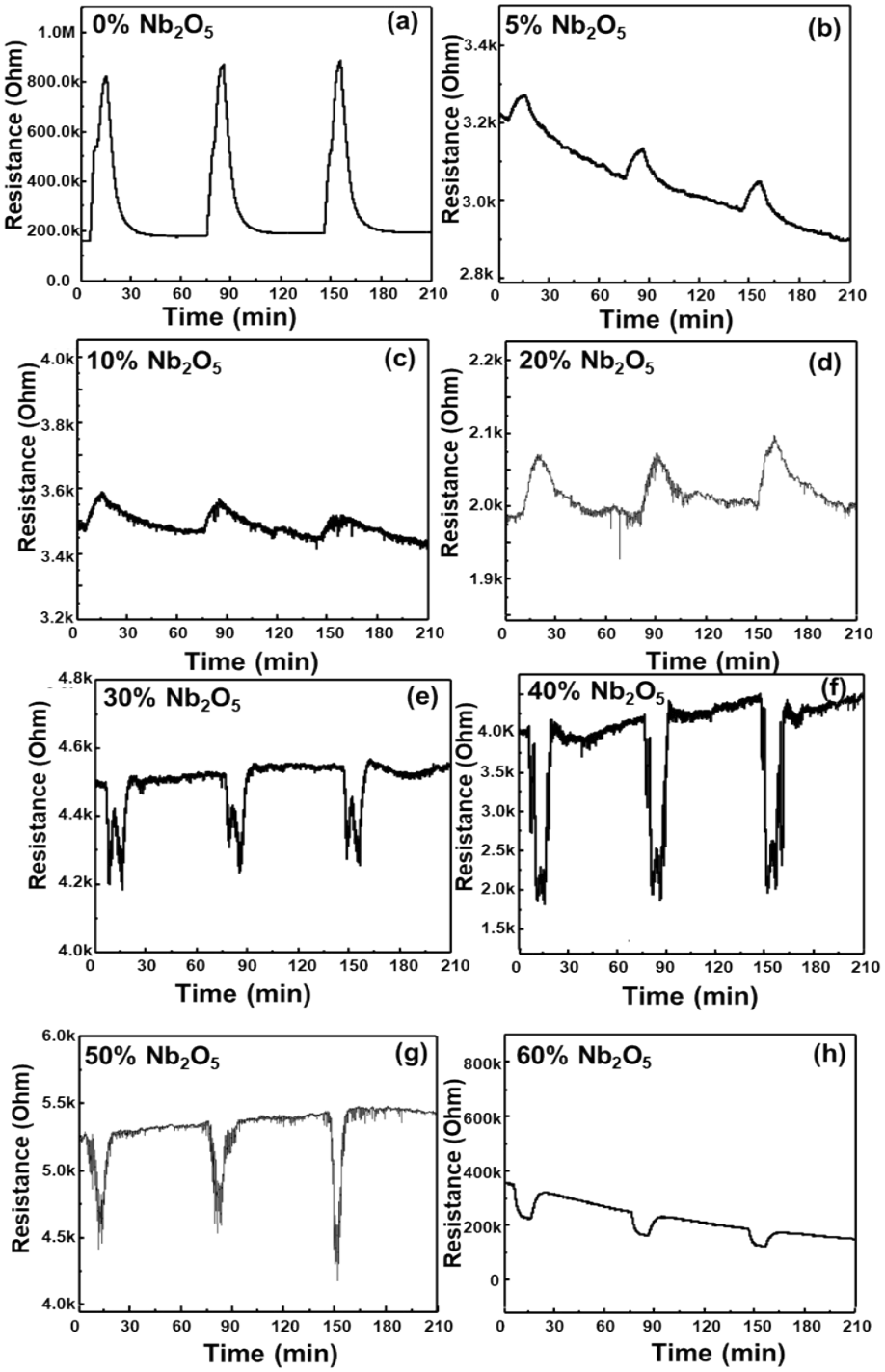

Figure S5: Gas sensing characteristics with different Nb_2O_5 concentration tested sensing device at 220°C temperature towards 500 ppb H_2S (a) 0%, (b) 5%, (c) 10%, (d) 20%, (e) 30%, (f) 40%, (g) 50%, (h) 60% loading of Nb_2O_5.

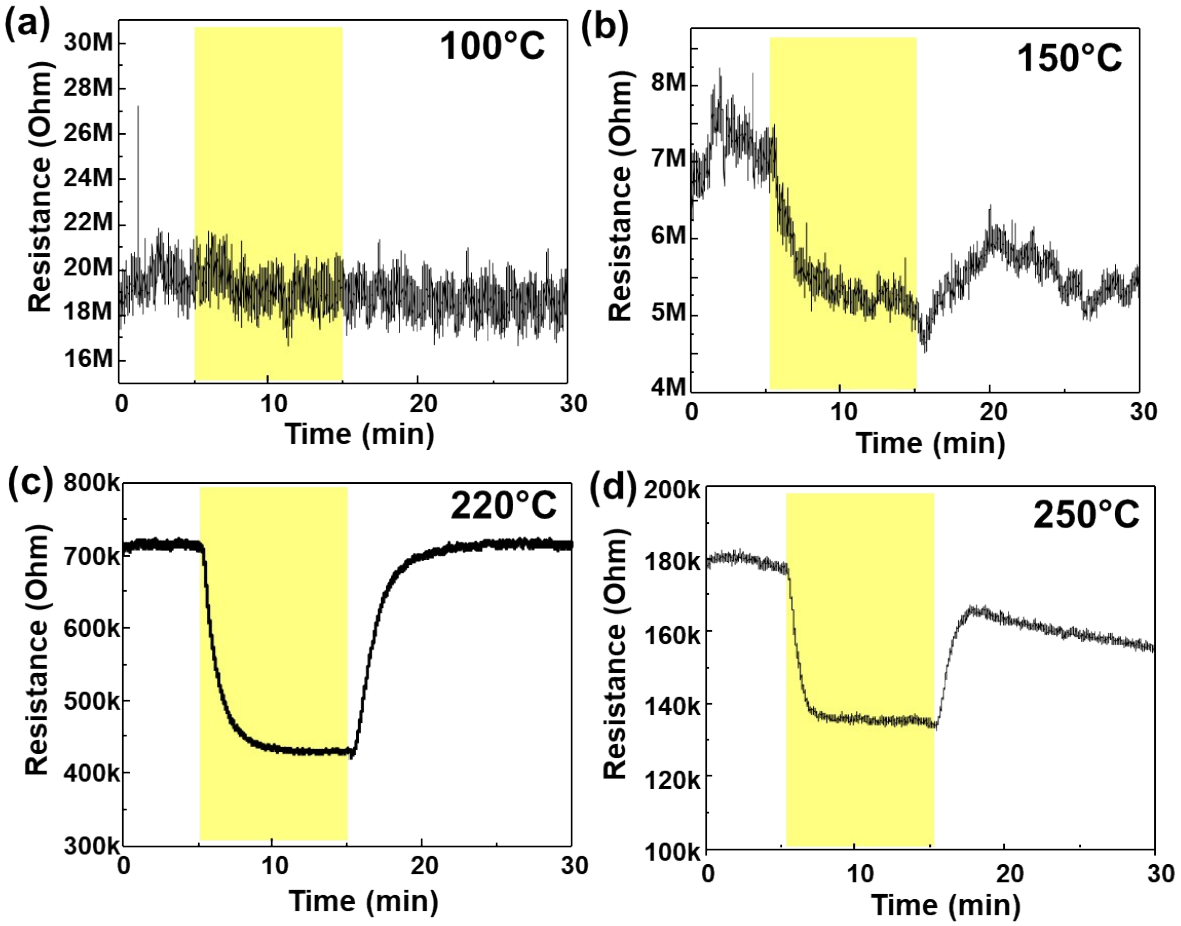

Figure S6: H_2S gas sensing of pure Nb_2O_5 at different temperature (a) 100°C (b) 150°C, (c) 220°C, (d) 250°C.

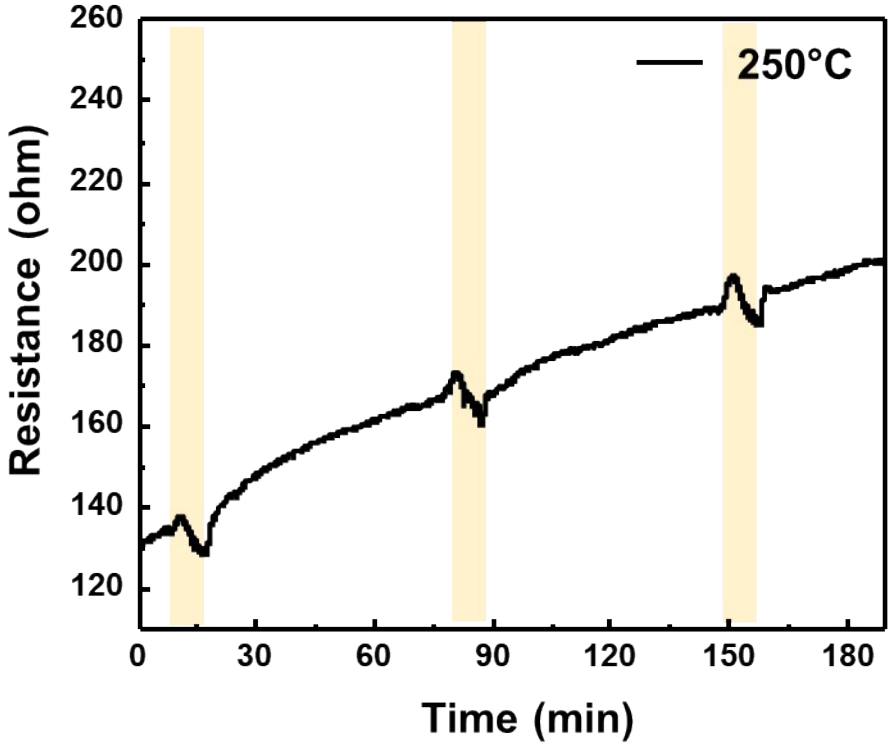

Figure S7: three repetitive cycles of H_2S gas sensing of CuO-Nb_2O_5 at 250°C temperatures.

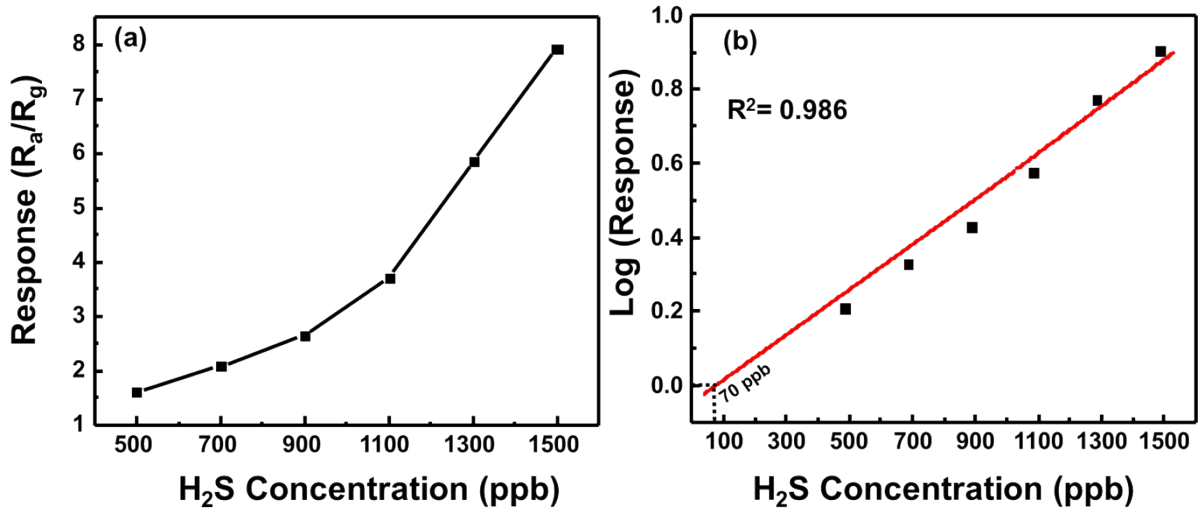

Figure S8: response versus gas concentration (H_2S) as sensitivity of CuO–Nb_2O_5 at 220°C temperatures (a) linear response, (b) log response.

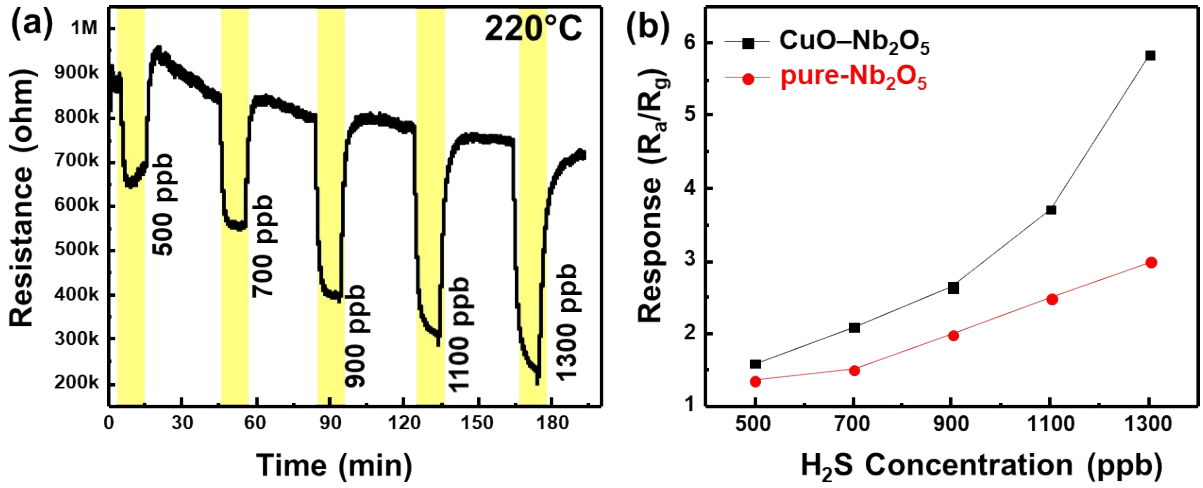

Figure S9: (a) H_2S gas sensing of pure Nb_2O_5 at different H_2S concentration, (b) response valve of pure Nb_2O_5 and CuO– Nb_2O_5 at different H_2S concentration.

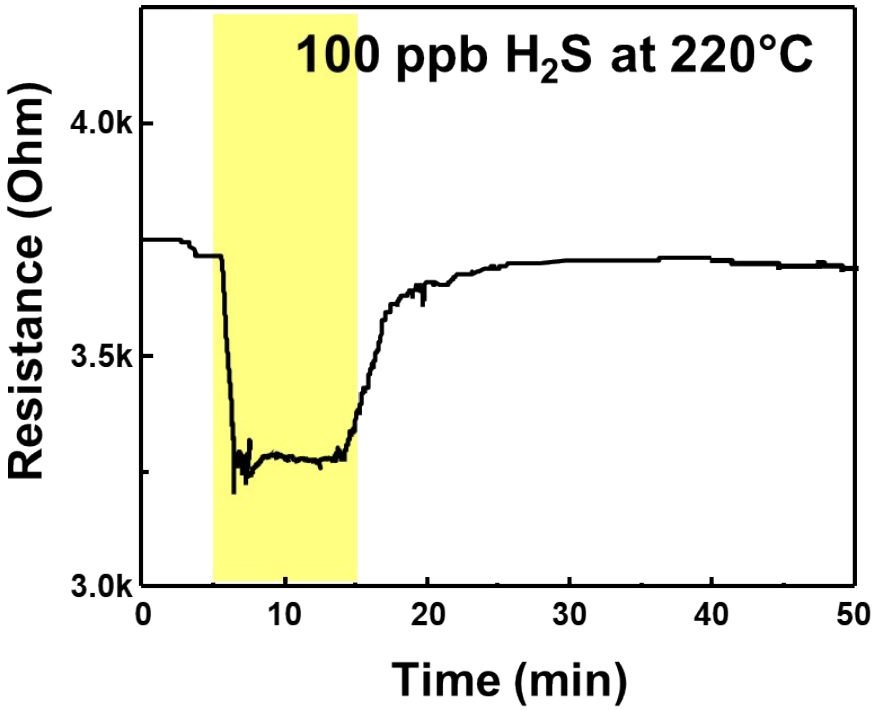

Figure S10: CuO– Nb_2O_5 sensor gas response at 100 ppb H_2S gas at 220°C.

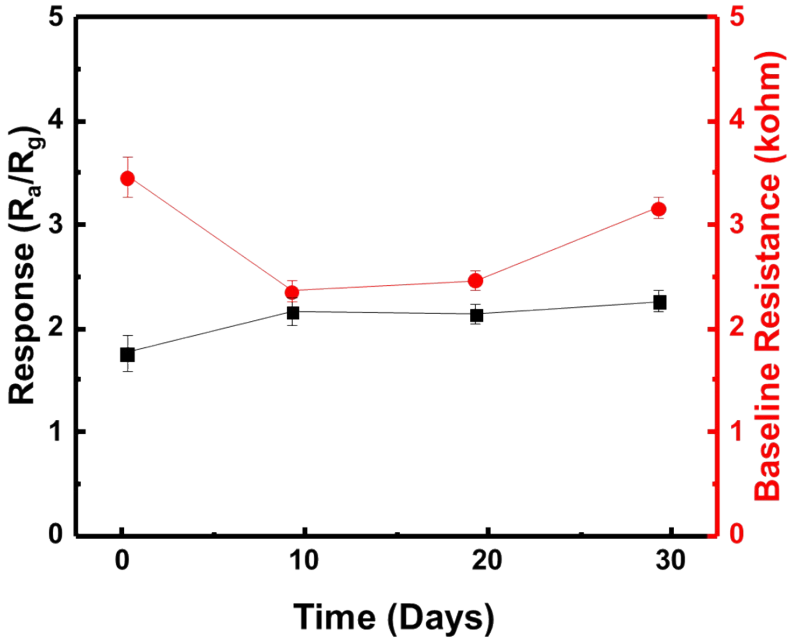

Figure S11: the change of response value and baseline resistance with time for CuO– Nb_2O_5 sensor at 220℃ during 500 ppb H_2S exposure.

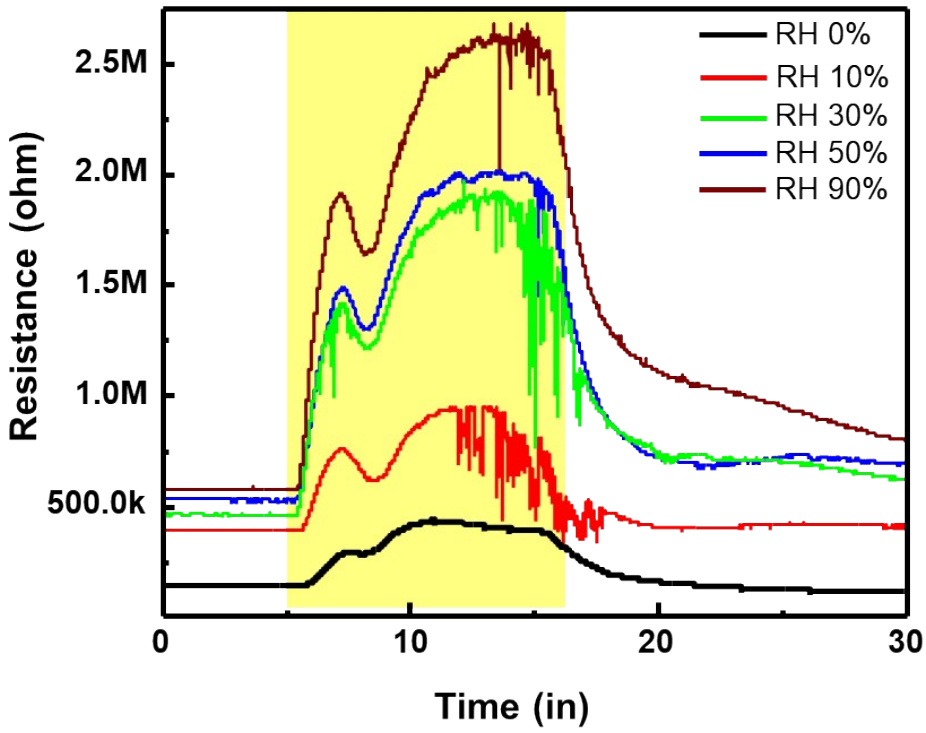

Figure S12: Gas response of CuO sensor toward 500 ppb H_2S as a function of relative humidity from 0 to 90% at 220°C.

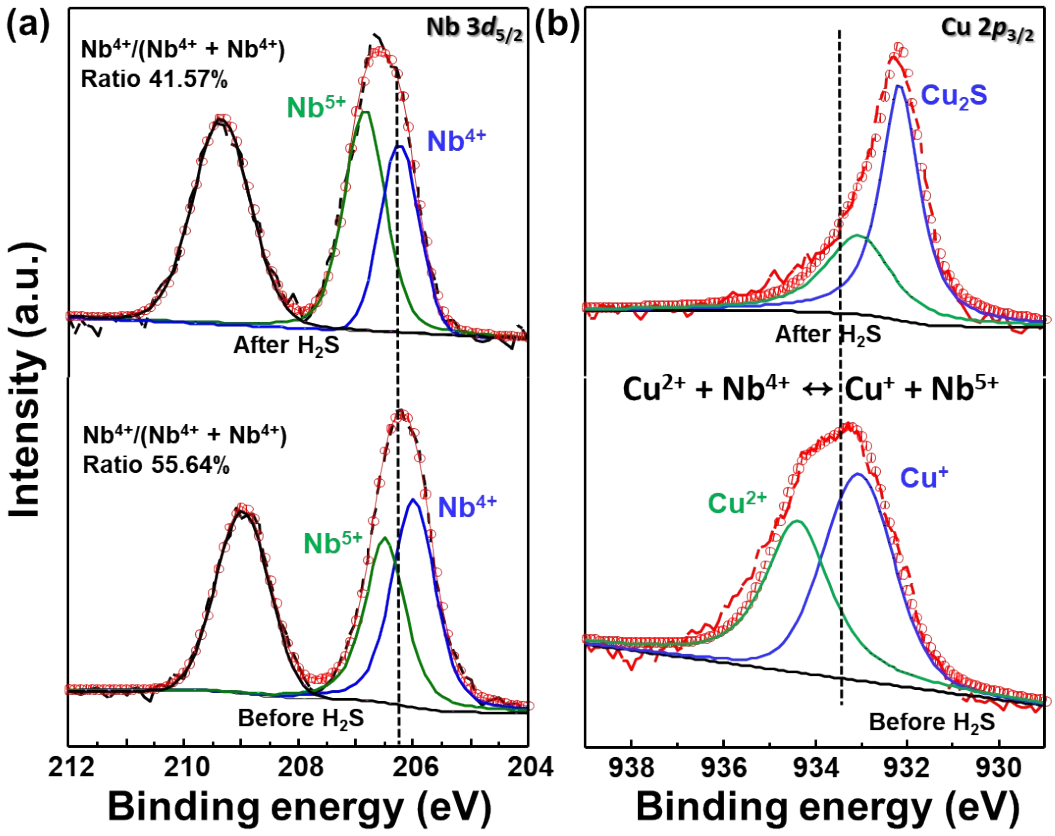

Figure S13: Deconvoluted XPS spectra of CuO-Nb_2O_5 before and after H_2S exposure (a) Nb 3*d*, (b) Cu 2*p*.

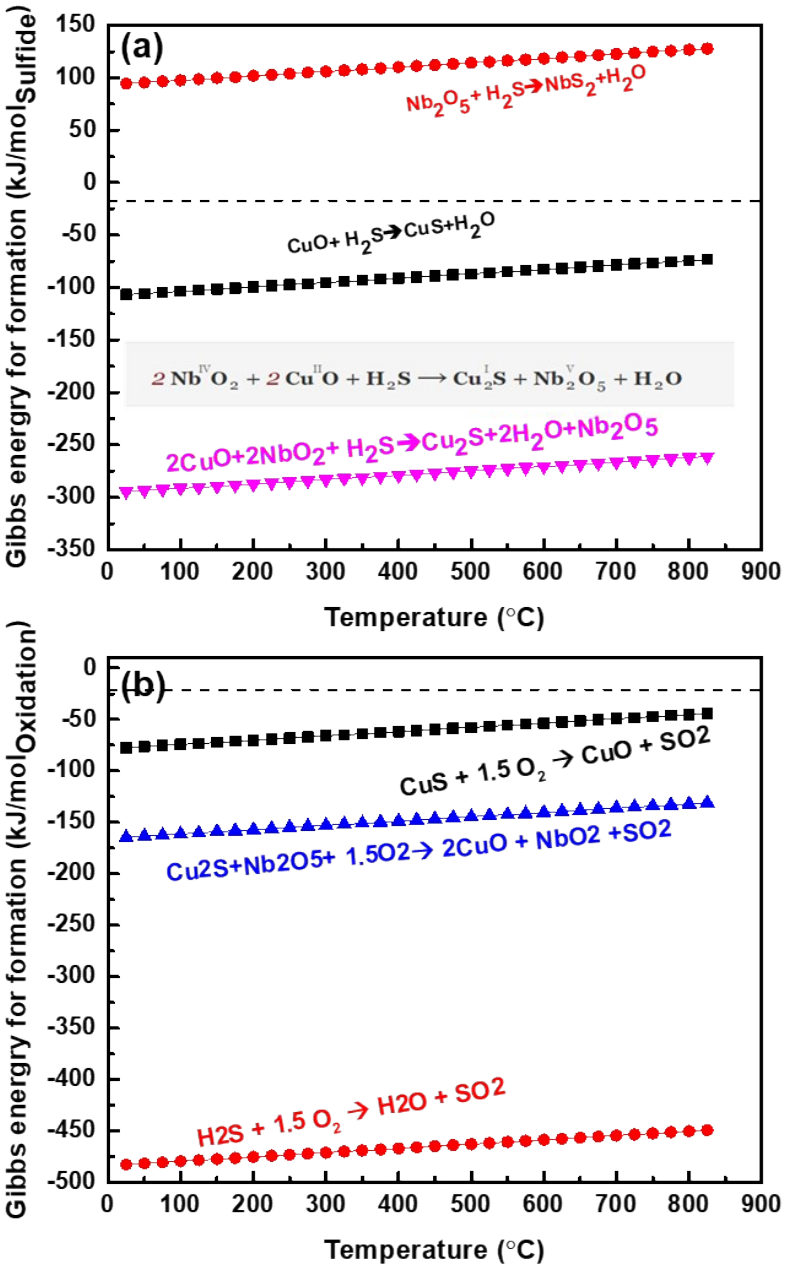

Figure S14: Thermodynamic Gibbs free energy of formation of (a) sulfidation reaction, (b) oxidation reaction using H_2S and O_2 gas.

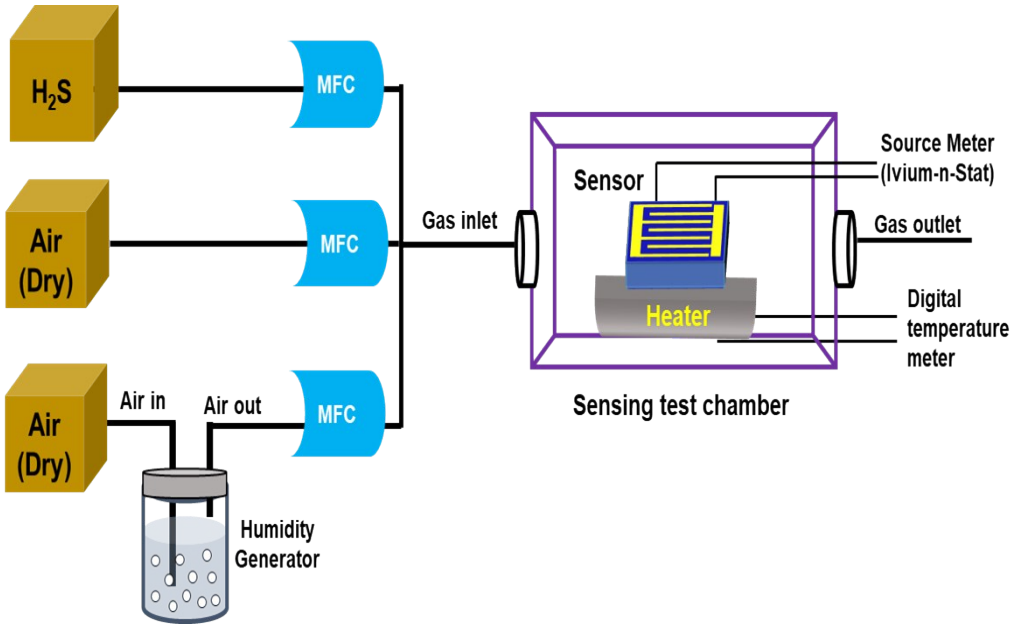

Figure S15: Schematic diagram of the lab-made humidity sensor measurement system.

Table S1: Calculated sensing response time and recovery time of CuO-Nb_2O_5 sensor.

Temperature (°C)	Response time (min)	Recovery time (min)
100	10	>20 min
150	10	>15 min
160	8	>15 min
180	7	>15 min
200	5	10 min
220	3	1 min

Table S2: state of the art: various reported studies for H_2S sensing where H_2S directly reacts with the CuO to generate metallic CuS.

Materials	Sulfidation Temp. (°C)	Oxidation temp. (°C)	Response (Conc.)
CuO encapsulated in SiO_2[1]	160	350	8 (10 ppm)
CuO monolayer[2]	25	300	8 (10 ppm)
CuO encapsulated in SiO_2[3]	160	350	-- (-- ppm)
CuO/In_2O_3[4]	70	400	229.3 (5 ppm)
CuO microflowers[5]	25	300	2 (1 ppm)
WO_3/CuO composites[6]	80	300	105 (5 ppm)
Pd doped CuO nanoflower[7]	80	300	123 (50 ppm)
Pt-doped CuO[8]	40	300	135.1 (10 ppm)
Our work (Nb_2O_5-CuO)	160-220	160-220	9 (1.5 ppm)

References

[1] A. Paul, B. Schwind, C. Weinberger, M. Tiemann, T. Wagner, *Adv. Funct. Mater.* **2019**, *29*, 1904505.
[2] Z. Xu, Y. Luo, G. Duan, *ACS Appl. Mater. Interfaces* **2019**, *11*, 8164.
[3] A. Paul, C. Weinberger, M. Tiemann, T. Wagner, *ACS Appl. Nano Mater.* **2019**, *2*, 3335.
[4] S. Li, L. Xie, M. He, X. Hu, G. Luo, C. Chen, Z. Zhu, *Sensors Actuators B Chem.* **2020**, *310*, 127828.
[5] K. Wu, C. Zhang, *J. Mater. Sci. Mater. Electron.* **2020**, 1.
[6] M. He, L. Xie, X. Zhao, X. Hu, S. Li, Z.-G. Zhu, *J. Alloys Compd.* **2019**, *788*, 36.
[7] X. Hu, Z. Zhu, C. Chen, T. Wen, X. Zhao, L. Xie, *Sensors Actuators B Chem.* **2017**, *253*, 809.
[8] Q. Tang, X.-B. Hu, M. He, L.-L. Xie, Z.-G. Zhu, J.-Q. Wu, *Appl. Sci.* **2018**, *8*.